

2011

Improvement of Rock Bolt Profiles using Analytical and Numerical Methods

Chen Cao

University of Wollongong, chen_cao@uow.edu.au

Jan Nemcik

University of Wollongong, jnemcik@uow.edu.au

Naj Aziz

University of Wollongong, naj@uow.edu.au

Follow this and additional works at: <https://ro.uow.edu.au/coal>

Recommended Citation

Chen Cao, Jan Nemcik, and Naj Aziz, Improvement of Rock Bolt Profiles using Analytical and Numerical Methods, in Naj Aziz and Bob Kininmonth (eds.), Proceedings of the 2011 Coal Operators' Conference, Mining Engineering, University of Wollongong, 18-20 February 2019
<https://ro.uow.edu.au/coal/350>

IMPROVEMENT OF ROCK BOLT PROFILES USING ANALYTICAL AND NUMERICAL METHODS

Chen Cao, Jan Nemcik and Naj Aziz

ABSTRACT: The anchorage capacity of fully grouted bolts has been studied for many years, however the bolt rib profile and its effect on bolt shear resistance is poorly understood. A new development in calculating load transfer capacity between two rib profiles of varying geometries is discussed. The derived mathematical equations presented calculate the stress distribution adjacent to the fully grouted bolt and bolt pull out force needed to fail the resin. The Fast Lagrangian Analysis Continua (FLAC) program was used to verify the calculations of stress within the resin. The novel idea of coupling the bolt geometry with the calculated stress provides another powerful tool to investigate the bolt profile configuration and its effects on the load transfer mechanism for the benefit of the mining industry.

INTRODUCTION

Steel bolts are an essential part of roadway support in coal mining roadways. The effectiveness of bolt reinforcement is a well known and well researched subject; however, little has been done in optimising the bolt profile that directly contributes to the load transfer between the bolt and the surrounding resin. To improve bolt load transfer through the steel rebar design, it is essential to research the details of the bolt profile shape and configuration. Analytical studies, laboratory tests and numerical modelling provide the tools that enable a better understanding of the rebar profile role in increasing the shear resistance during the working life of bolts.

Investigations of load transfer between the bolt and resin indicates that the bolt profile shape and spacing plays an important role in improving the shear strength between the bolt and the surrounding strata. The short encapsulation pull out tests of rock bolt indicate significant variance of shear resistance for various bolt profile spacing, angle, shape and size. Empirical studies can match the graphs of physical tests however these methods cannot describe the exact reasoning why such behaviour occurs. Numerical modelling techniques are much better as they can mimic the physical tests in great detail; however, these methods depend on an accurate knowledge of the physical properties that must be incorporated or added into the model. For example, in the micro-scale world resin properties may not be the same as those indicated in the laboratory tests. The power of the numerical model rests on its ability to compare several models and to establish the optimum solution to the problem. The laboratory testing has its challenges as fabrication of minute differences in bolt profile in the workshop is difficult. Nevertheless the laboratory tests are important to calibrate all the empirical work and the numerical models. At present a mathematical description of the bolt profile and its behaviour during the bolt pull out test is under development to provide better understanding of the physical process that influence the shear strength of the loaded bolt.

The *in situ* pullout tests are commonly used to examine the shear capacity of rock bolts. Only a few researchers (Blumel, *et al.*, 1997 and Aziz, *et al.*, 2008) have conducted laboratory tests to study various bolt profile parameters and their influence on the bolt anchorage. A typical steel bolt profile configuration is shown in Figure 1. Aziz *et al.* (2008) found out that the shear load capacity and stiffness vary greatly for various bolt profile configurations and showed that the bolts with profile spacing (PS) of 12.5 mm exhibit very low stiffness while spacing of 37.5 mm had higher peak and residual strengths. The results are presented in Figure 2. Other experimental tests by Aziz and Webb (2003) indicated that smooth bolts exhibit very low shear resistance.

Clearly, the mathematical description of the physical problem provides an understanding of the bolt profile behaviour and together with the numerical modelling would constitute a realistic approach to improving the bolt rib profile configuration which is the subject of this study.

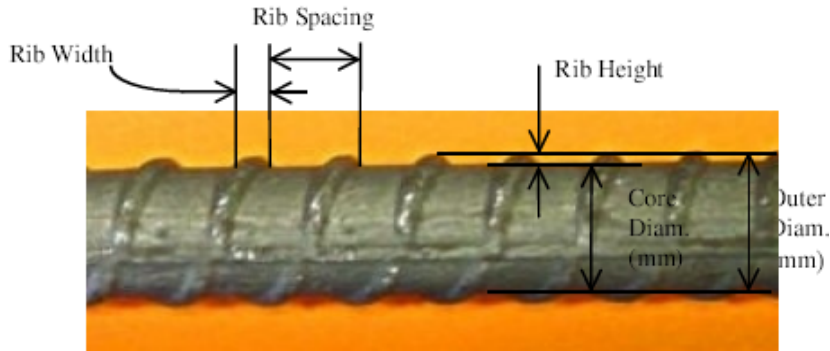


Figure 1 - Steel bolt rib profile configuration

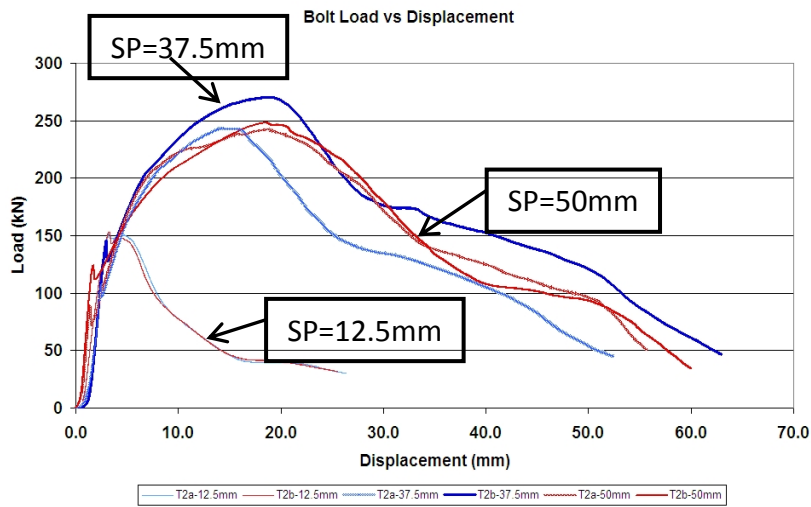


Figure 2 - Laboratory studies of steel bolt pull out tests versus the maximum load for various bolt rib profile spacing (after Aziz *et al.*, 2008)

STRESS DISTRIBUTION IN INFINITE ELASTIC MEDIA

Derived mathematical equations enable calculations of the stress tensor at any point within the resin encapsulating the loaded steel bolt. Such detail can make assessment of the bolt profile and its influence on the shear strength possible. Boussinesq (Poulos and Davis, 1974) derived fundamental solutions for various loads on infinite or semi-infinite elastic media.

While loading an infinite strip on the surface of a semi-infinite mass as shown in Figure 3, the stress tensor anywhere within the media can be calculated as a function of the load, position and material properties. For a uniform normal load as shown in Figure 3, the stress tensor can be calculated using the Boussinesq equations while for the uniform shear load, the stress distribution can also be calculated via Cerutti's equations (Poulos and Davis, 1974).

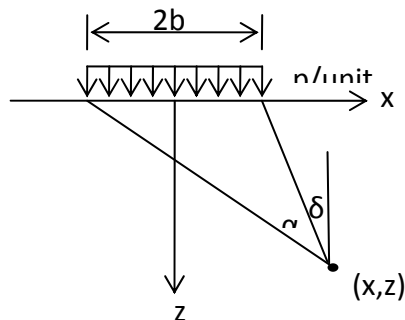


Figure 3 - Calculated stress tensor at any position given by x and z coordinates within the semi-infinite elastic medium loaded by a uniformly distributed load (p)

MODELLING OF STRESS DISTRIBUTION ADJACENT TO THE BOLT PROFILE

To draw a link between the load transfer system and the bolt profile configuration, a single spacing between two bolt ribs is examined (Figure 4).

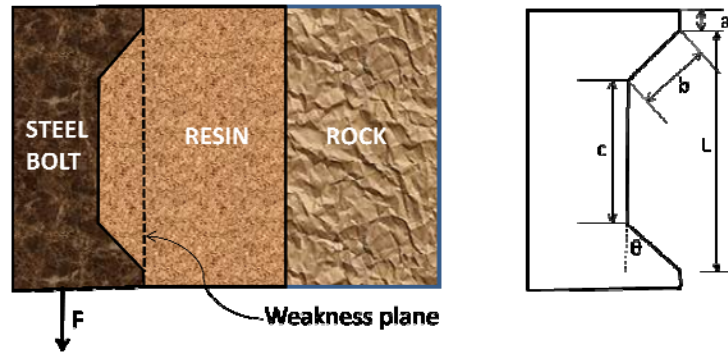


Figure 4 - A single spacing between two bolt profiles showing geometry

When the bolt is loaded, the load is applied to the resin boundary as shown in Figure 5. The location of these loads is dependent on the bolt geometry while their magnitudes depend on the bolt geometry and the resin-bolt interface properties. During the bolt pull out tests, the loads can be shown as shear forces and normal forces as shown in Figure 5.

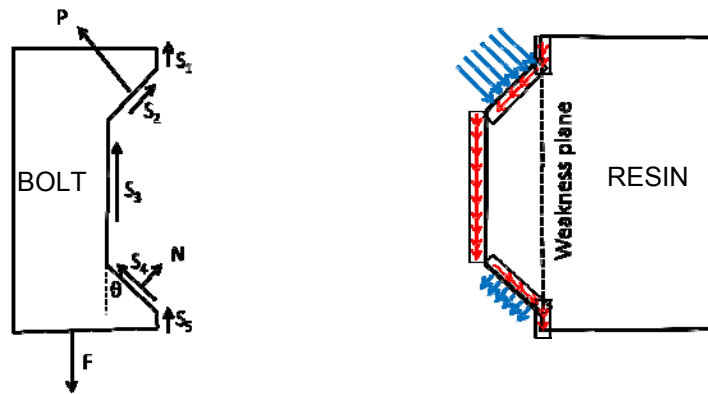


Figure 5 - Load transfer between the bolt and the resin

An assumption was made that the resin-bolt interface forces S_1 , S_3 , S_4 and S_5 are small and when the angle θ approaches 90° the shear force S_2 becomes small thus, all shear forces at the interface are equal to zero.

The stress at the bolt interface can therefore be assumed to be as shown in Figure 6a where the normal stress remains acting along the side of the bolt profile. This stress component plays a major role in stress distribution within the resin.

A FLAC model was used to validate this simplification. The model simulated a section of the steel bolt shown in Figure 6b with the angle $\theta = 45^\circ$. The pull out force was applied to the bolt and the modelled shear stress contours were plotted as shown in Figure 6b. The modelled contours were compared with the shear stress calculated using the Boussinesq and Cerutti's equations. Both the calculated and modelled contours were in reasonable agreement indicating that the numerical assumptions can be used. Properties used in the calculations and in the FLAC model are shown in Table 1.

Table 1 - Material properties used in calculations and FLAC model

UCS (MPa)	71
Shear strength (MPa)	16.2
E (GPa)	12
Poisson ratio	0.25

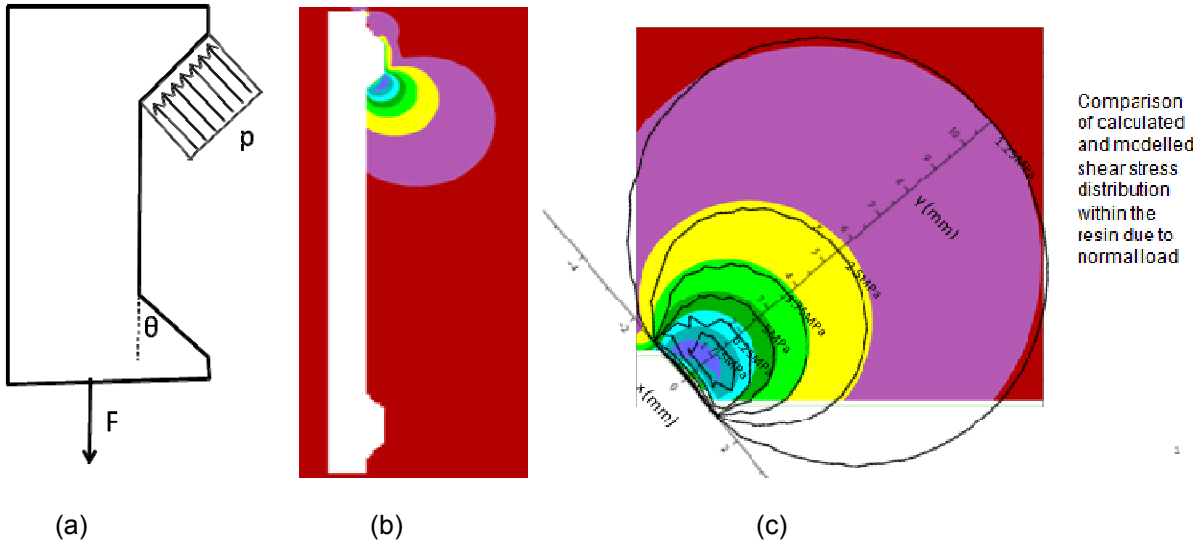


Figure 6 - Bolt profile geometry (a) Comparison of calculated and modelled shear stress (b and c)

NORMAL AND SHEAR STRESS ON A FAILURE PLANE

To investigate where the resin failure will occur, several potential planes of failure can be trialled. As an example a plane of failure that spans between the two rib tops is considered. The Mohr-Coulomb criterion of failure was used to calculate the maximum pull out force needed for the assumed plane of failure.

The equations to calculate the bolt pull out force are derived after linking the bolt geometry shown in Figure 4 and the sum of integrated normal and shear stresses along the failure plane. The lengthy mathematics of the stress tensor solutions and sums of forces along the plane of failure are not presented here, and are outside the scope of this paper. The Matlab program designed for numerical solutions of complex problems was also introduced to obtain specific solutions where derivation of mathematical equations was too complex.

For static equilibrium, the sum of forces parallel to the bolt axis is zero:

$$\sum F_y = 0$$

If the shear forces are assumed to be very small than from Figure 5a:

$$\therefore F = pb \sin \theta, \text{ and: } p = \frac{F}{b \sin \theta}$$

Where, F = axial bolt pull out force;

p = Normal load on bolt boundary at the profile inclination b.

STRESS DISTRIBUTION IN THE RESIN

The FLAC modelling indicates that the evenly distributed compressive load (p) has the major influence on the stress in the resin while all interface shear and tensile stresses are small and can be ignored.

To apply Boussinesq's stress transformation equations in calculating the normal and shear stress along the studied plane of failure, the coordinate system must be rotated to match the geometry shown in Figure 3. The rotation is shown in Figure 7 where the distance PQ represents the failure plane and the angle theta is the rib slope. Point (A) is any point on the plane of failure while variable (h) is the distance from point P.

Under normal conditions the resin elastic properties are similar to the surrounding strata and the resin boundary can be extended to infinity.

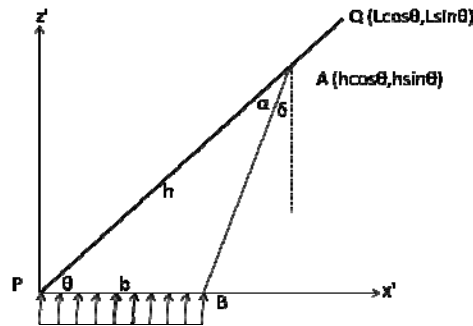


Figure 7 - Rotated axis of the loading diagram with the assumed plane of failure

The stress tensor transformation calculations using the Boussinesq equations transform stress to shear and normal stress along the failure plane PQ (Figure 7). To be able to calculate changes in normal and shear stress parallel to the failure plane when the bolt geometry changes, the bolt profile dimensions must be coupled with the stress within the equations. The angles α and δ shown in Figure 7 need to be substituted with bolt profile configuration parameters a , b , c and θ shown in Figure 4. To simplify derivation of the mathematical equations, this step is done after stress transformation.

The normal and shear stress to the failure plane are determined after stress transformation, lengthy integrations, rearrangement and substitutions of each term. The final solutions are as follows:

$$\int \sigma_n dh = \frac{F}{b\pi \sin \theta} \left[\left(\frac{\pi}{2} - \theta \right) (c + 3b \cos \theta) - (c + 2b \cos \theta) \tan^{-1} \left(\frac{c \cos \theta + b \cos 2\theta}{c \sin \theta + b \sin 2\theta} \right) + b \cos \theta \tan^{-1} \left(\frac{c + b \cos \theta}{b \sin \theta} \right) \right]$$

And the sum of shear forces to the failure plane is:

$$\int \tau dh = \frac{p}{\pi} \int \sin^2 \alpha dh = \frac{F}{\pi} \left[\tan^{-1} \left(\frac{c + b \cos \theta}{b \sin \theta} \right) + \frac{\pi}{2} - \theta \right]$$

MOHR-COULOMB FAILURE STUDY ALONG THE PLANE OF WEAKNESS

Two combined stress fields are considered within the resin. The first one is the initial pre-loading stress tensor at the failure surface and the second one is the load induced stress tensor. Due to bolt installation procedure, the initial pre-loading stress, within the resin, is considered to be small as most of the resin along the bolt cures after pre-tensioning the bolt.

Thus, the failure criterion (f) is expressed as net resistant force that can be summed up as:

$$f = (c_w + \mu \sigma_{n0} - \tau_0)L + \left(\int \mu \sigma_n dh - \int \tau dh \right)$$

Where:

$L = c + 2b \cos \theta$ = failure length; h = distance from any chosen point along the plane of weakness from 0 to L ; c_w = cohesion; $\mu = \tan \phi$, where ϕ is an internal angle of friction of the resin; σ_{n0} = initial normal stress; τ_0 = initial shear stress; τ = shear stress introduced by pull out force; and b , c and θ are bolt profile parameters.

The forces along the plane of weakness are shown in Figure 8, and the failure criterion expression can be written as:

$$f = c_w L + L \mu \sigma_{n0} - L \tau_0 + \mu \int \sigma_n dh - \int \tau dh$$

Substituting integrated solutions into the equation:

$$f = F_0 + \frac{F \mu}{\pi b \sin \theta} \left[\left(\frac{\pi}{2} - \theta \right) \left(c + 3b \cos \theta - \frac{b \sin \theta}{\mu} \right) - (c + 2b \cos \theta) \tan^{-1} \left(\frac{c \cos \theta + b \cos 2\theta}{c \sin \theta + b \sin 2\theta} \right) + b \left(\cos \theta - \frac{\sin \theta}{\mu} \right) \tan^{-1} \left(\frac{c + b \cos \theta}{b \sin \theta} \right) \right]$$

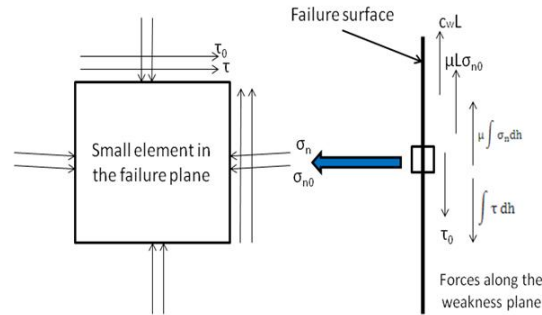


Figure 8 - Forces on a small element and along the plane of weakness

APPLICATION EXAMPLE

In this example, let failure length $L=10$ mm and $c = 8.5$ mm as constants. Rib height, $b\sin\theta$, varies from 0 to 4 mm shown in Figure 9 as coloured line (All dimensions in Figure 9 are in mm).

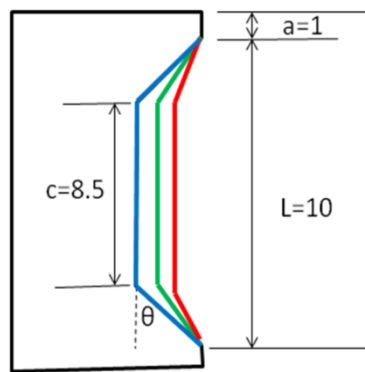


Figure 9 - Application example, failure length L is 10 mm, c is 8.5mm and rib height varies from 0 to 4 mm

For initial conditions, let:

$$\sigma_{n0} = 0 \text{ MPa and } \tau_0 = 0 \text{ MPa}$$

For material properties, let resin cohesion $c = 16$ MPa and frictional angle $\phi = 35^\circ$. Then

$$F_0 = L(c_w + \mu\sigma_{n0} - \tau_0) = 10(16 + \tan 35^\circ \times 0 - 0) = 160 \text{ N}$$

Using failure criteria formula:

$$f = F_0 + \frac{F\mu}{\pi b \sin \theta} \left[\left(\frac{\pi}{2} - \theta \right) \left(c + 3b \cos \theta - \frac{b \sin \theta}{\mu} \right) - (c + 2b \cos \theta) \tan^{-1} \left(\frac{c \cos \theta + b \cos 2\theta}{c \sin \theta + b \sin 2\theta} \right) + b \left(\cos \theta - \frac{\sin \theta}{\mu} \right) \tan^{-1} \left(\frac{c + b \cos \theta}{b \sin \theta} \right) \right]$$

$$= 160 + F \cdot G(\theta)$$

Where F is bolt pull-out force.

The $G(\theta)$ may be called the “ influence factor” of the rib height. If the influence factor is positive, the failure will never occur on the assumed plane of weakness. If the influence factor is negative, the failure may occur on the weakness line within the resin. In addition, while the influence factor is negative, the larger the absolute value of the influence factor, the easier the failure propagates.

The plot of $G(\theta)$ versus rib height ($b\sin\theta$) is shown in Figure 10.

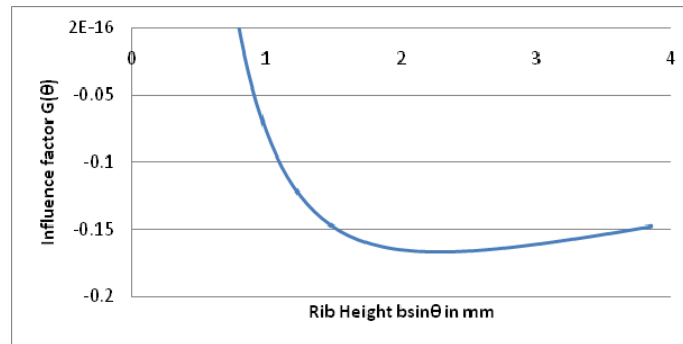


Figure 10 - Influence factor versus rib height

From the graph in Figure 10 it can be concluded that:

- The minimum rib height is about 0.8 mm to initiate a failure on the proposed plane of weakness. If the rib height is less than 0.8 mm, then $G(\theta) \geq 0$, and

$$f = 160 + F \cdot G(\theta) \geq 0.$$
 It means that failure will never happen on the proposed weakness line.
- The minimum influence factor $G(\theta) \approx -0.17$ when the rib height is about 2mm. Therefore the minimum bolt pull out force to cause the resin failure is

$$F = 160/0.17 = 941 \text{ N}$$
- For any other rib height the probability of failure along the proposed weakness plane decreases.

CONCLUSIONS

The study of the bolt profile shape presented shows how the mathematical equations were derived. These equations are used to calculate the pull out force needed to fail the resin for different bolt profile configuration. The calculations can be applied to any plane of probable failure within the resin. The important outcome of this study is to show that there is another way to examine resin failure around the bolt for different profile configurations that can be compared with the laboratory tests and numerical modelling. This method can provide better understanding of the bolt-resin interaction with rock reinforcement.

The derived mathematical equations consist of in-built bolt geometry parameters and these can be changed to optimise the bolt shear strength capacity. Various types and bolt geometries and profile configurations can be trialled using the described approach. This method provides another step towards designing more efficient bolt profiles to optimise the support capacity in the mining industry. Future efforts will be made to extend the calculations to three dimensions while the final outcome of this work is to write a computational program to evaluate the pull out force for various bolt profile geometries..

REFERENCES

- H Poulos and E Davis, 1974. Elastic solutions for rock mechanics. *Textbook by John Willey and Sons, Inc.* New York. TA710.P67, 624.1513, 73-17171, Printed in New York.
- Blumel, M, Schweger, H F and Golser, H, 1997. Effect of rib geometry on the mechanical behaviour of grouted rock bolts. *World Tunnelling Congress '97, 23rd General Assembly of the International Tunnelling Ass.* Wien. 6 p.
- Aziz, N I and Webb, B, 2003. Study of load transfer capacity of bolts using short encapsulation push test, *Proc. 4th Underground Coal Operators Conference, Coal 2003, February 12-14, Wollongong*, pp 72-80. <http://ro.uow.edu.au/coal/162/>.
- Aziz, N I, Jalalifar H and Concalves, J, 2006. Bolt surface configurations and load transfer mechanism, *Proc. 7th Underground Coal Operators Conference, Coal 2006, Wollongong, 5-7 July*, pp. 236-244. <http://ro.uow.edu.au/coal/51/>.
- Aziz, N I, Jalalifar, H, Remennikov, A, Sinclair, S, Green, A, 2008. Optimisation of the Bolt Profile Configuration for Load Transfer Enhancement, in *Proceedings of 8th Underground Coal Operators' Conference* (Eds: N Aziz and J Nemcik), February 14-15, Wollongong, pp 125-131. <http://ro.uow.edu.au/coal/11/>.